Journal of Nuclear Materials 377 (2008) 438–443

Contents lists available at ScienceDirect

Journal of Nuclear Materials

journal homepage: www.elsevier.com/locate/jnucmat

Atomistic modeling of the vibrational and thermodynamic properties of uranium dioxide, UO_2

Prabhatasree Goel *, N. Choudhury, S.L. Chaplot

Solid State Physics Division, Bhabha Atomic Research Centre, Trombay, Mumbai 400 085, India

ARTICLE INFO

Article history:
Received 14 August 2007
Accepted 10 March 2008

PACS:
66.30.Hs
63.20.Dj
65.40.2b

ABSTRACT

Modeling the thermal properties of uranium oxide is of immense interest to the nuclear industry. UO_2 belongs to the family of superionic conductors whose solid-state diffusion coefficients at high temperatures are comparable to that of liquids. We report lattice dynamics and molecular dynamics studies carried out on oxide UO_2 in its normal as well as superionic phase. Lattice dynamics calculations have been carried out using shell model in the quasiharmonic approximation. The calculated equilibrium structure, elastic constants, bulk modulus, phonon frequencies and specific heat are in excellent agreement with the reported experimental data. Pressure variation of the phonon dispersion and equation of state have also been predicted. Molecular dynamics simulations have been carried out to study the diffusion behavior and the thermodynamic properties in UO_2. The diffusion constant of O in UO_2 has been determined. The pair correlation functions, O–U–O bond angle and thermal amplitude of vibration for the oxygen atom provide a microscopic picture of the local structure thereby throwing light on the gradual increase in the disorder of the oxygen sub-lattice which is a signature of superionic transition. The calculated transition temperature of UO_2 is 2300 K, which compares well with experimental value of about 2600 K.

© 2008 Elsevier B.V. All rights reserved.

1. Introduction

UO_2 is an important material for nuclear industry. It is the usual fuel used for pressurized heavy water reactors. Knowledge of the thermodynamic and transport properties of nuclear fuel at high temperatures is of great interest [1–7]. A clear understanding of its thermophysical [8–25] properties is of utmost need for its various applications. It also belongs to the class of oxide fast-ion conductors [1,18–24], which allow macroscopic movement of ions through their structure. Rapid diffusion of a significant fraction of one of the constituent species occurs within an essentially rigid framework of other species. In UO_2, it is the uranium, which forms the rigid framework while superionic conduction arises from massive disorder of the oxygen sub-lattice. The study of phonon spectra and lattice vibrations is of particular interest because several physical properties of crystals like their specific heat, thermal expansion, thermal conductivity, phase transitions, melting, transmission of sound, optical properties and interaction with radiations such as X-rays and neutrons are all related to the vibrations of atoms in solids.

Microscopic modeling [26] or simulation is necessary to understand the conduction processes at high temperatures in these crystals. Uranium dioxide exhibits the fluorite structure having space group *Fm3m* [27]. Uranium atoms form a face centered cubic network, all tetrahedral sites of which are occupied by oxygen atoms. This compound shows a type-II superionic transition attaining high levels of ionic conductivity following a gradual and continuous disordering process within the same phase [1,2,5]. Several theoretical and experimental works have been reported on numerous fast-ion conductors like Li_2O, CaF_2, BaF_2, PbF_2, $SrCl_2$, CuI, etc., [28]. The main impetus for these studies has been to unravel the causes behind the process of fast-ion conduction. In case of UO_2, interest has been manifold owing to its use in the nuclear field. The high temperature studies in UO_2 have been motivated by its use as a nuclear fuel for nuclear fission reactors. This oxide behaves similar to other superionic halides. The extensive diffusion is characterized by a large decrease in the elastic constant C_{11} [2,19,29,20] and specific heat anomaly at the transition temperature, T_c. Neutron scattering measurements indicate that the anionic sub-lattice in UO_2 becomes heavily disordered in the region of 2300 K [2,3,19,30]. Measured elastic constants [2,3,29] do show a softening above 2400 K in the region where fast-ion behavior is expected in UO_2, but the variation below this temperature is already very large. There is a high increase in specific heat [31–39] at high temperatures in UO_2. Its behavior complies with the general belief that fluorites in general show a diffuse transition at about 0.8 T_m (T_m = melting point, T_m of UO_2 is 3120 K). Above the transition temperature the diffusion coefficient of one of the constituent atom becomes comparable to that of liquids [1]. Detailed study of the processes

* Corresponding author.
E-mail address: knp@barc.gov.in (P. Goel).

0022-3115/$ - see front matter © 2008 Elsevier B.V. All rights reserved.
doi:10.1016/j.jnucmat.2008.03.020

occurring in the crystal lattice at elevated temperatures is essential to understand the transitions.

In the present study, we have developed interatomic potentials which have been used to derive the crystal structure, elastic properties phonon spectra and thermodynamic properties. Extensive reported experimental data validate the model which has been used for deriving various high-pressure–temperature properties of UO_2. Molecular dynamics simulations are aimed at understanding the mechanism of diffusion. Section 2 presents the details of the comprehensive lattice dynamics calculations. Section 3 deals with the details of the molecular dynamics simulations. Section 4 summarizes and discusses the numerous results obtained using both the techniques. Section 5 gives the various inferences concluded from this study.

2. Lattice dynamics calculations

Our calculations have been carried out in the quasiharmonic approximation [40,41] using the interatomic potentials consisting of Coulomb and short-range Born–Mayer type interaction terms as in our earlier studies [28,42–44],

$$V(r_{ij}) = \frac{e^2}{4\pi\varepsilon_0}\frac{Z(k)Z(k')}{r_{ij}} + a\exp\left[\frac{-br_{ij}}{R(k)+R(k')}\right], \quad (1)$$

where, r_{ij} is the separation between the atoms i and j of type k and k', respectively. $R(k)$ and $Z(k)$ are the effective radius and charge of the kth atom, a and b are the empirical parameters optimized from several previous calculations [42–44]. Oxygen atoms have been modeled using a shell model, where a massless shell of charge $Y(k)$ is linked to the atomic core by harmonic force constant $K(k)$. Lattice constant, zone center phonon frequencies and elastic constants have been fitted to experimental values. The final set of optimized parameters used in the calculation is given in Table 1. The calculations have been carried out using the current version of the software DISPR [45] developed at Trombay. The interatomic potential enables the calculation of the phonon frequencies in the entire Brillouin zone.

Group theoretical symmetry analysis was undertaken to classify the phonon modes belonging to various representations. Because of the selection rules only phonon modes belonging to certain group theoretical representations are active in typical single crystal Raman, infrared and inelastic neutron scattering measurements. These selection rules are governed by the symmetry of the system and the scattering geometry employed. The theoretical scheme for the derivation of the symmetry vectors is based on irreducible multiplier representations [46] and construction of symmetry adapted vectors, which are used for block diagonalizing the dynamical matrix [44]. These permit the assignment of the phonon modes belonging to various representations. For UO_2, group theoretical analysis provides a classification of the frequencies at zone center (Γ-point) and the high symmetry directions (Δ, Σ and Λ), into the following representations:

Γ: $2T_{1u} + T_{2g}$ where T_{1u} and T_{2g} phonon modes are triply degenerate

(00ζ): $2\Delta_1 + \Delta_2 + 3\Delta_3$,
$(\zeta\zeta 0)$: $3\Sigma_1 + 2\Sigma_2 + \Sigma_3 + 3\Sigma_4$,
$(\zeta\zeta\zeta)$: $3\ \Lambda_1 + 3\Lambda_3$,

Table 1
Model parameters (a = 1822 eV, b = 12.364)

Atom type (k)	$R(k)$ (nm)	$Z(k)$	$Y(k)$	$K(k)$ (eV/nm^{-2})
Uranium	0.21	2.90e	–	–
Oxygen	0.175	−1.45e	−2	11000

where the Λ_3 and Δ_3 phonon modes are doubly degenerate. Based on the crystal symmetry, UO_2 is expected to have one infrared active mode (T_{1u}) and one Raman active optical mode (T_{2g}). The classifications of the phonon modes into different irreducible representations enable direct comparison with single crystal Raman, infrared and neutron data.

Phonon density of states is an integrated average over all phonon modes in the complete Brillouin zone. It is defined by the equation

$$g(\omega) = c\int_{BZ}\sum_j \delta(\omega - \omega_j(\mathbf{q}))d\mathbf{q}, \quad (2)$$

where, c, is a normalization constant, such that $\int g(\omega)d\omega = 1$, $\mathbf{q}$ is the reduced wave vector in the Brillouin zone, ω_j is the frequency of the jth phonon mode. The phonon density of states is the key quantity required to derive various thermodynamic properties [44]. The phonon density of states of UO_2 has been calculated by effectively integrating over a $4\times4\times4$ mesh of wave vectors in the cubic reciprocal space unit cell while taking advantage of the symmetry of the Brillouin zone. The contribution from individual atom species can be obtained as partial density of states, which is given as

$$g_k(\omega) = c\int\sum_j |\xi(\mathbf{q}j,k)|^2\delta(\omega-\omega_j(\mathbf{q}))d\mathbf{q}, \quad (3)$$

where, ξ ($\mathbf{q}j$, k) is the polarization vector of the phonon $\omega_j(\mathbf{q}j)$. The calculated density of states can be used to evaluate the various thermodynamic properties of the solid including specific heat at constant volume, which is given as

$$C_V(T) = k_B\int\left(\frac{\hbar\omega}{kT}\right)^2\frac{e^{\frac{\hbar\omega}{k_BT}}}{\left(e^{\frac{\hbar\omega}{k_BT}}-1\right)^2}g(\omega)d\omega. \quad (4)$$

To compare with experimental data, we need to calculate $C_P(T)$, which is given as

$$C_P(T) = C_V(T) + \alpha_v(T)^2BVT, \quad (5)$$

where, bulk modulus,

$$B = -V(dP/dV). \quad (6)$$

The volume coefficient of thermal expansion is given as,

$$\alpha_v(T) = \frac{1}{BV}\sum_i \Gamma_i C_{v_i}(T); \quad i = \mathbf{q}j, \quad (7)$$

Γ_i is the Gruneisen parameter for the jth phonon mode at wave vector $\mathbf{q}$ and is given by

$$\text{Gruneisen parameter}, \quad \Gamma_i = -\frac{\partial\ln\omega_i}{\partial\ln V}. \quad (8)$$

Using the Lyddane–Sachs–Teller (LST) relations [47], we have estimated

$$\frac{\varepsilon_0}{\varepsilon_\infty} = \frac{\omega_{LO}^2}{\omega_{TO}^2},$$

where, ε_0 and ε_∞ are respectively, the zero and the high-frequency dielectric constants, while ω_{LO} and ω_{TO} are the longitudinal optic and transverse optical phonon frequencies.

3. Molecular dynamics simulation

Molecular dynamics is a powerful method for exploring the structure and dynamics of solids, liquids and gases. Explicit computer simulation of the structure and dynamics using this technique allows microscopic insights into the behavior of materials to understand the macroscopic phenomenon like diffusion of

oxygen ions and their contribution to the fast-ion transition, in this case. An interatomic potential, which treats U and O as rigid units may be sufficient to study properties like diffusion. The optimized parameters obtained from lattice dynamics studies have been used for these simulations. In our study, we have taken a macro-cell of 1500 rigid atoms with periodic boundary conditions to study the response of the system when set free to evolve from a configuration disturbed from the equilibrium situation. The lattice parameters and atomic trajectories can thus be obtained as a function of temperature and external pressure [48–51]. Calculations in this work have been done using the software developed at Trombay [45]. The simulations have been done at various temperatures up to and beyond the fast-ion transition. The diffusion coefficient, mean square displacement of oxygen ion and the pair correlation functions were calculated to understand the local environment in the normal as well as the superionic phase and to understand the changes taking place upon transition.

The pair correlation function of a crystal consisting of various atoms at a given r is dependent on

$$g_{k'k}(r) \propto \frac{1}{4\pi r^2} \sum_{i,j}^{i\neq j} \delta\{r - r_{ij}(kk')\}, \tag{9}$$

where, $r_{ij}(kk')$ is the separation between the positions of ith and jth constituent atoms while k and k' refer to the different kinds of atoms. Molecular dynamics simulations have been carried out at various temperatures starting from 300 K to 3000 K at zero pressure and studied over timesteps of 20 000 fs. The diffusion of uranium and oxygen ions has been monitored.

Table 2
Comparison between calculated and experimental lattice [1,19] parameters and elastic constants at ambient conditions

Physical quantity	Experimental	Calculated
Lattice parameter (nm)	0.5470(1)	0.546
Bulk modulus (GPa)	207	181
C_{11} (GPa)	389(5)	387
C_{44}(GPa)	60(3)	66
C_{12} (GPa)	119(7)	77
Anisotropy factor ($2C_{44}/(C_{11}-C_{12})$)	0.426	0.444

Table 3
Comparison between the computed and experimental light scattering data and their corresponding Gruneisen parameters. The computed dielectric behavior $(\varepsilon_0/\varepsilon_\infty) = 4$ is underestimated as compared to the experimental [52,53] value of 5.14

Mode	Experiment wavenumber (cm^{-1})	Calculated wavenumber (cm^{-1})	Γ_i (expt. [53])	Γ_i (calc.)
T_{1u}(LO)	556	576	0.52	0.65
T_{1u} (TO)	278	254	1.83	2.58
T_{2g}	431	468	1.28	1.18

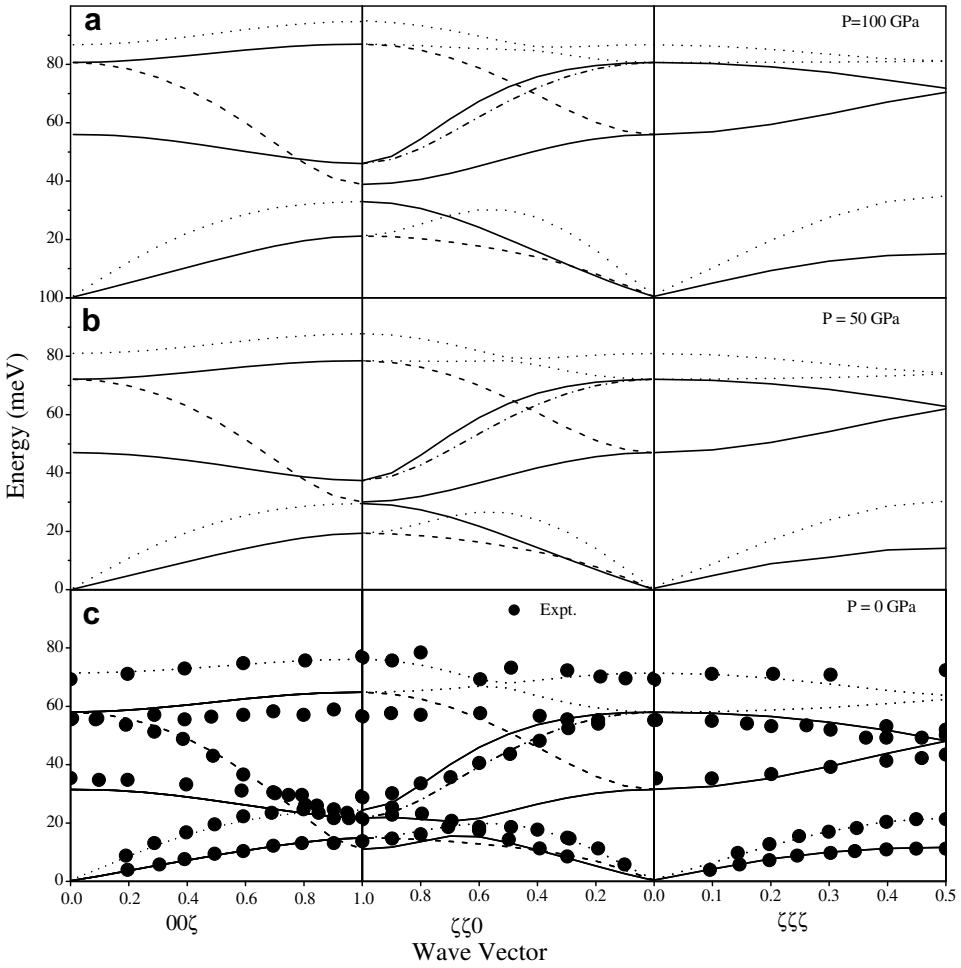

Fig. 1. Calculated (full lines) phonon dispersion relation in UO_2; (a) $P = 0$ GPa. (b) $P = 50$ GPa. (c) $P = 100$ GPa. The $P = 0$ GPa calculated dispersion relations are compared with reported (solid circles) experimental inelastic neutron scattering data (Dolling et al. [54]).

4. Results and discussions

4.1. Phonon spectra and thermodynamic properties of UO_2

The calculated values of the lattice parameter, bulk modulus, and elastic constants compare well with the experimentally obtained data [52,53] as given in Table 2. The values of the optically active Raman and infrared frequencies and their Gruneisen constants are given in Table 3. The average Gruneisen constant, Γ_i for all the phonons in uranium oxide is 1.55. The computed ratio of zero and high-frequency dielectric constant $\varepsilon_0/\varepsilon_\infty$ is in satisfactory agreement with experiments. The calculated Gruneisen constant of the LO mode is found to be substantially lower than that of the TO mode, as observed experimentally [53].

The phonon dispersion relation in UO_2 at various pressures, is shown in Fig. 1, along the various high symmetry directions. The computed dispersion at $P = 0$ GPa is in excellent agreement with available inelastic neutron scattering experimental data [54]. The phonon frequencies are found to harden progressively with increasing pressure. With increase in pressure, our calculations do not indicate any softening of the phonon modes. Theoretical studies reveal a free energy crossover at about 70 GPa [42]. The present detailed phonon dispersion relation calculations indicate that this transition is not driven by dynamical instabilities but arises due to the lower volume of the high-pressure cotunnite phase. At $P = 0$ GPa, the highest phonon branch is seen at about 70 meV, which shifts up to 80 meV at $P = 50$ and further to 80 meV at $P = 100$ GPa. The energy spread between the acoustic modes is greater at higher pressures. The gap between the lowest optic mode and the highest acoustic mode increases with increasing pressure at the zone boundary.

The total and partial densities of UO_2 are given in Fig. 2. The observations of phonon dispersion picture are further substantiated by this figure. The energy span at $P = 0$ GPa is between 0 and 70 meV, at $P = 50$ GPa it is up to 80 meV, while at $P = 100$ GPa it spans up to 90 meV. The peaks in the phonon spectra progressively harden with increase of pressure. The partial densities of states of the oxygen atoms show that they contribute almost throughout the range mainly from 20 to 70 meV at lowest pressure, between 40 and 80 meV at 50 GPa and between 50 and 90 meV at 100 GPa. Uranium atoms's predominant contribution is limited to the lower energy range up to 25 meV and its position remains unchanged with pressure, indicating its much higher stability as compared to the oxygen atoms.

Fig. 3(a) gives the computed specific heat $C_P(T)$ compared to reported data [37,55]. Quasiharmonic lattice dynamics calculations significantly underestimate the observed specific heat (full line in Fig. 3(a)). Taking into account the thermal expansion values obtained from molecular dynamics simulations and temperature variation of bulk modulus, fairly accurate description of the C_P–C_V corrections are obtained. The computed specific heat at high temperature after incorporating these corrections (open circles in Fig. 3(a)) are in good agreement with experiments [37] and reported molecular dynamics simulations of Yakub et al. [55]. There are various factors like disordering of the oxygen sub-lattice, electronic excitations, valence- conduction band transitions, etc., which play a significant role in the anomalous increase in the specific heat which sets in even before the fast-ion transition. The estimated Frenkel defect energy of UO_2 [42] involving formation of an oxygen vacancy/interstitial pair was found to be ~4.1 eV, in good agreement with reported first principles [56] and experimental data [57]. Defects do not contribute significantly over the 0–1600 K temperature range reported in this study, but divalent Frenkel defects are the predominant form of atomic disorder [58]. The equation of state is shown in Fig. 3(b), however, experimental data for the same is unavailable for comparison. There is a smooth decrease in volume with increase in pressure.

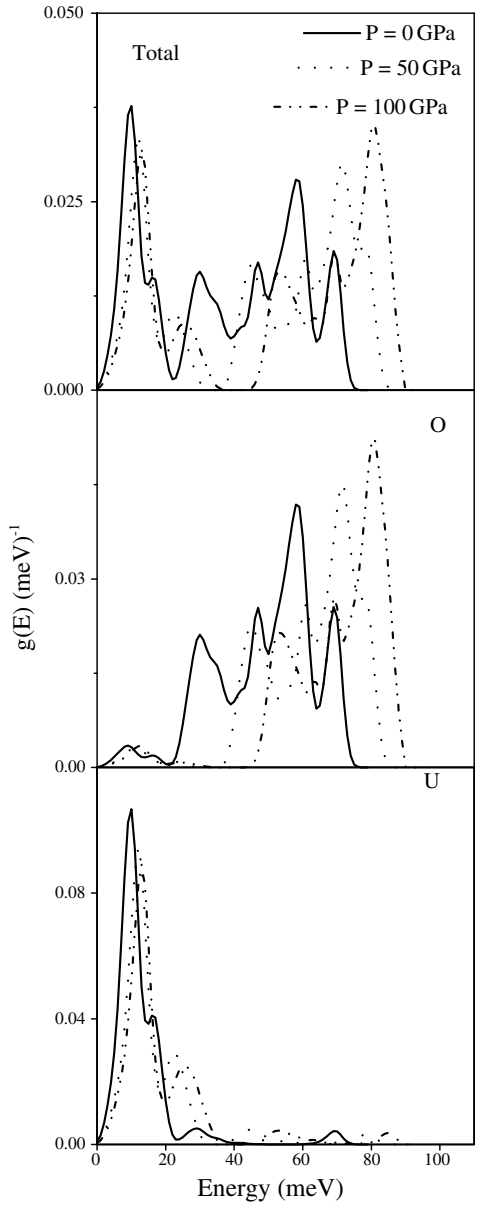

Fig. 2. Phonon density of states at $P = 0$ GPa; $P = 50$ GPa; $P = 100$ GPa along with the partial density of states for uranium and oxygen as calculated by quasiharmonic lattice dynamics calculations.

4.2. Diffusion and fast-ion transition

The diffusion coefficient of the oxygen ion has been computed as depicted in Fig. 4. High temperature data of the diffusion constant of oxygen in UO_2 is unavailable for comparison. Our molecular dynamics calculations suggest that the superionic phase sets around 2300 K, results have been compared and are found to be in good agreement with those of Yakub et al. [55]. The signature of a superionic transition is found indirectly in the enthalpy studies on UO_2, since direct measurements are made difficult with high temperatures involved [31–39]. It is found to undergo a *bredig* transition (involving jump in specific heat across the normal to superionic phase transition) at about 2610 K. The diffusion coefficient is comparable to that of a liquid in the superionic phase.

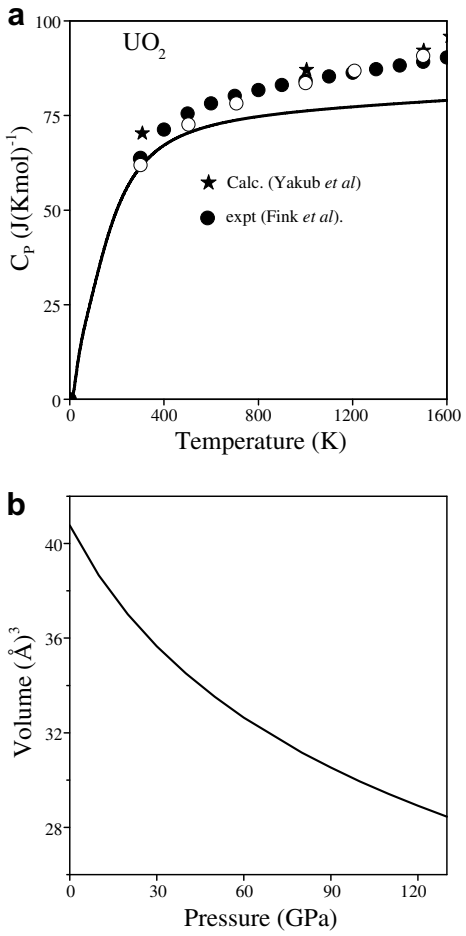

Fig. 3. (a) Calculated specific heat at constant pressure, $C_P(T)$. Quasiharmonic lattice dynamics (full line) significantly underestimate the observed $C_P(T)$ (solid circles (Fink et al. [37])). Taking into account the thermal expansion values obtained from molecular dynamics simulations and temperature variation of bulk modulus, a fairly accurate description of $C_P(T)$ has been obtained (open circles) which are in good agreement with experimental data [37] as well as reported molecular dynamics results (Yakub et al. [55]). (b) The calculated equation of state for UO_2.

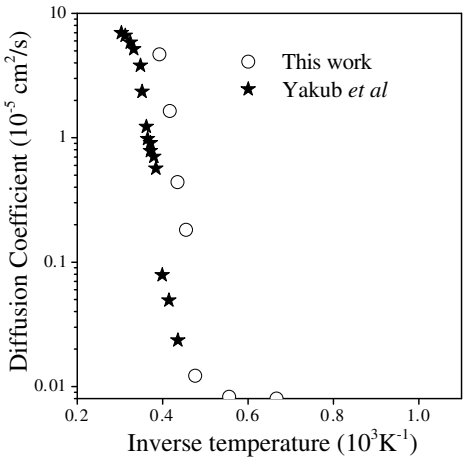

Fig. 4. Oxygen atom's diffusion coefficient, D and its variation with temperature obtained from MD simulations in comparison with those reported by Yakub et al. [55].

Calculations of the thermal amplitude using molecular dynamics simulations (open circles) have been compared with experimental results [2] and reported calculations [55] in Fig. 5(a), and

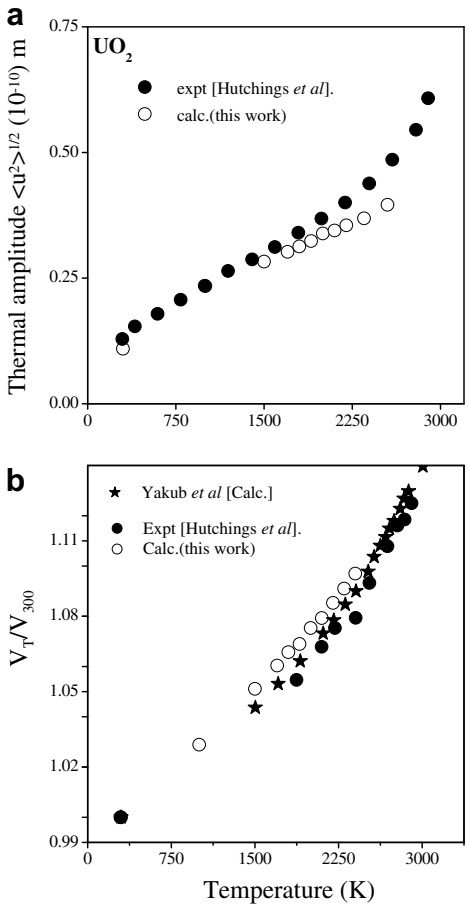

Fig. 5. (a) Calculated (MD simulations) thermal amplitude of oxygen $\langle u^2 \rangle^{1/2}$ as a function of temperature (open circles) at ambient pressure and comparison with experiment (solid circles) (Hutchings et al. [2]). (b) Variation of lattice volume with temperature at ambient pressure, compared with experimental [2] (solid circles) and reported molecular dynamics (solid stars, Yakub et al. [55]) results. Open circles, as derived from molecular dynamics simulations, denote calculated values in this work.

is in good agreement. The change in the slope of the plot at the superionic transition ($T \sim 2300$ K) is seen clearly. The thermal expansion of the unit cell obtained from the MD simulations, which includes anharmomic effects is plotted in Fig. 5(b), agrees well with experiment. In case of the reported experiment [2], the various data points correspond to different crystals and different instruments.

The information on the nearest neighbour distances can be obtained from the radial pair correlation functions. The pair correlation of the UO_2 lattice at different temperature from $T = 300$ K (room temperature) to superionic state at $T = 2550$ K is plotted in Fig. 6(a). Gradual disordering of the oxygen sub-lattice can be seen with increasing temperature. In the U–U correlation, we can see that there are very little changes in the peak positions. The plots at various temperatures almost overlap completely. We can conclude that the U–U order is almost untouched by the growing thermal disturbances. In case of U–O, little but subtle changes can be seen with increase in temperature. But the maximum changes are seen in the O–O pair correlation, the peaks broaden with temperature increase and at highest temperature investigated, the probability of finding an oxygen atom is nonzero at any point beyond a minimum distance. Similarly, the angle-correlation changes in the O–U–O reveal more fluctuations and a broader character as temperature is raised. From the above discussion we can conclude that the disturbances in the crystal

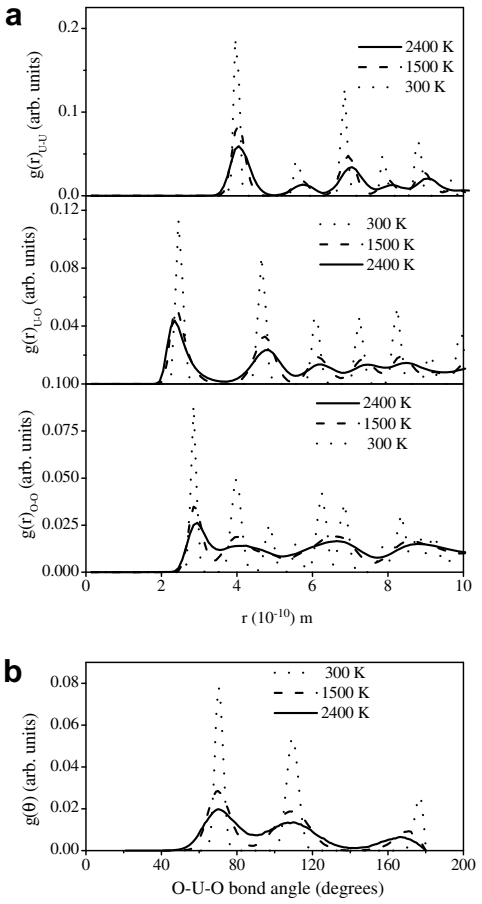

Fig. 6. (a) Pair correlation functions of U–U, U–O and O–O and (b) angle-correlation function of O–U–O bond angle in UO_2 at different temperatures and ambient pressure as obtained from MD simulations.

lattice accompanying the superionic transition are limited to the oxygen sub-lattice alone.

5. Conclusions

A shell model has been successfully used to study the phonon properties of uranium dioxide. The interatomic potential is able to reproduce the elastic constants, bulk modulus, equilibrium lattice constant, and phonon frequencies, which are in good agreement with the reported data. The calculated phonon dispersion relation is in very good agreement with the reported neutron scattering data. There is no phonon softening in UO_2 even up to high-pressures of 100 GPa. Partial densities of state of uranium and oxygen atoms show that they contribute almost in the whole energy span up to 75 meV. There is a greater contribution of oxygen in the higher energy side as compared to uranium, which contributes more on the lower end. This may be explained with regards to their size and mass. The calculated specific heat is in good agreement up to about 1200 K but shows a slower rise as compared to the experimental data beyond which several other factors like crystal field effects, electronic transitions, defect formation, etc., start to play role.

The diffusion coefficient calculated for oxygen ion shows a transition to the fast-ion phase at around 2300 K whereas in experiment, it is seen to occur around 2670 K. At the transition temperature, oxygen atom's diffusion coefficient is comparable to that of a liquid and is in the order of 10^{-9} m^2/s. The pair correlation functions for U–U, U–O and O–O and the angle distribution for O–U–O bring out the following inferences. The pair correlations for O–O just show a gradual broadening with increase in temperature from 300 K to 2550 K. The distortions in the lattice due to fast-ion diffusion are highly localized, and the local environment remains unchanged to a great extent. As a result, the lattice seems more or less undisturbed. The interatomic potential formulated for UO_2 may be transferred to other similar actinide dioxides oxides like ThO_2, PuO_2, etc., with suitable modifications to study their vibrational and thermodynamic properties.

References

[1] S. Hull, Rep. Prog. Phys. 67 (2006) 1233.
[2] M.T. Hutchings, J. Chemical Society Faraday Trans. 283 (1987) 1083.
[3] K. Clausen, W. Hayes, M.T. Hutchings, J.E. Macdonald, R. Osborn, P.G. Schnabel, Phys. Rev. Lett. 52 (1984) 1238.
[4] J.C. Ramirez, M. Stan, P. Cristea, J. Nucl. Mater. 359 (2006) 174.
[5] D. Manara, C. Ronchi, M. Sheindin, R. Konings, J. Nucl. Mater. 362 (2007) 14.
[6] M. Freyss, T. Petit, J. Crocombette, J. Nucl. Mater. 347 (2005) 44.
[7] P.Y. Chevalier, E. FischerB. Cheynet, J. Nucl. Mater. 303 (2002) 1.
[8] V. Sobolev, J. Nucl. Mater. 344 (2005) 198.
[9] K.H. Kang, H.J. Ryu, K.C. Song, M.S. Yang, J. Nucl. Mater. 301 (2002) 242.
[10] J.K. Fink, J. Nucl. Mater. 279 (2000) 1.
[11] K. Govers, S. Lemehov, M. Hou, M. Verwerft, J. Nucl. Mater. 366 (2007) 161.
[12] H.Y. Geng, Y. Chen, Y. Kanita, M. Kinoshita, Phys. Rev. B 75 (2007) 054111.
[13] L.V. Matweev, M.V. Veshchunov, J. Nucl. Mater. 265 (1999) 285.
[14] D. Ippolito, L. Martinelli, G. Bevilacqua, Phy. Rev. B 71 (2005) 064419.
[15] I.D. Prodan, G.E. Scuseria, R.L. Martin, Phys. Rev. B 76 (2007) 033101.
[16] K. Ikushima, S. Tsutsui, Y. Haga, H. Yasuoka, R.E. Walstedt, N.M. Masaki, A. Nakamura, S. Nasu, Y. Onuki, Phys. Rev. B 63 (2001) 104404.
[17] C.J. Pickard, B. Winkler, R.K. Chen, M.C. Payne, M.H. Lee, J.S. Lin, J.A. White, V. Milman, D. Vanderbilt, Phys. Rev. Lett. 85 (2000) 5122.
[18] P.J.D. Lindan, M.J. Gillan, Philos. Mag. B 69 (1994) 535.
[19] K. Clausen, W. Hayes, M.T. Hutchings, J.K. Kjems, J.E. Macdonald, R. Osborn, High Temp. Sci. 19 (1985) 189.
[20] P. Sindzingre, M.J. Gillan, J. Phys. C: Solid State Phys. 21 (1988) 4017.
[21] C.B. Basak, A.K. Sengupta, H.S. Kamath, J. Alloys Compd. 360 (2003) 210.
[22] K. Kurosaki, Y. Kazuhiro, M. Uno, S. Yamanaka, K. Yamamoto, T.J. Namekawa, J. Nucl. Mater. 294 (2001) 160.
[23] P.J. Browning, J. Nucl. Mater 98 (1981) 345.
[24] V. Sobolev, S. Lemehov, J. Nucl. Mater. 352 (2006) 300.
[25] D.A. Keen, J. Phys.: Condens. Matter 14 (2002) R819.
[26] L.J. Porter, J. Li, S. Yip, J. Nucl. Mater. 246 (1997) 53.
[27] R.W.G. Wyckoff, Crystal Structures, 2nd Ed., Wiley, New York, 1965.
[28] P. Goel, N. Choudhury, S.L. Chaplot, Phys. Rev. B 70 (2004) 174307 and references therein.
[29] O.W. Brandt, T. Walker, Phys. Rev. Lett. 18 (1967) 11.
[30] K. Clausen, W. Hayes, J.E. Macdonald, P.G. Schnabel, M.T. Hutchings, J.K. Kjems, High Temp. High Press. 15 (1983) 383.
[31] C. Ronchi, G.J. Hyland, J. Alloys Compd. 213&214 (1994) 159.
[32] C. Ronchi, M. Sheindlin, M. Musella, G.J. Hyland, J. Appl. Phys. 85 (1999) 776.
[33] J. Ralph, G.J. Hyland, J. Phys.: Condens. Matter 132 (1985) 76.
[34] D.A. MacInnes, C.R.A. Catlow, J. Nucl. Mater. 89 (1980) 354.
[35] Hj. Matzke, J. Chemical Society Faraday Trans. 283 (1987) 1121.
[36] P. Browning, G. HylandJ. Ralph, High Temp. High Press. 15 (1983) 169.
[37] J.K. Fink, M.G. Chasanov, L. Leibowitz, J. Nucl. Mater. 102 (1981) 17.
[38] G.J. Hyland, J. Ralph, High Temp. High Press. 15 (1983) 179.
[39] J. Ralph, G.J. Hyland, J. Nucl. Mater. 132 (1985) 76.
[40] G. Venkatraman, L. Feldkamp, V.C. Sahni, Dynamics of Perfect Crystals, MIT, Cambridge, 1975.
[41] P. Bruesh, Phonons: Theory and Experiments, Springer Verlag, Berlin, 1986.
[42] P. Goel, N. Choudhury, S.L. Chaplot, J. Phys: Condens. Matter 19 (2007) 386239.
[43] K.R. Rao, S.L. Chaplot, N. Choudhury, S. Ghose, J.M. Hastings, L.M. Corliss, D.L. Price, Phys. Chem. Miner. 16 (1988) 83.
[44] S.L. Chaplot, N. Choudhury, S. Ghose, M.N. Rao, R. Mittal, P. Goel, Eur. J. Minerol. 14 (2002) 291.
[45] S.L. Chaplot, Report, 1978, BARC-972, 1992 (unpublished).
[46] O.V. Kovalev, Irreducible Representations of Space Groups, Gordan and Breach, NY, 1964.
[47] N.W. Ashcroft, N.D. Mermin, Solid State Physics, Harcourt College Publishers, 1976.
[48] S.L. Chaplot, K.R. Rao, Phys. Rev. B 35 (1987) 9771.
[49] S.L. Chaplot, Phys. Rev. B 42 (1990) 2149.
[50] S.L. Chaplot, N. Choudhury, Am. Mineral. 86 (2001) 752.
[51] S.L. Chaplot, Compos. Mater. Sci 37 (2006) 146.
[52] J.D. Axe, G.D. Petit, Phys. Rev. 151 (1966) 676.
[53] T. LivnehE. Sterer, Phys. Rev. B 73 (2006) 085118.
[54] C. Dolling, R. Cowley, A.D.B. Woods, Can. J. Phys. 43 (1965) 1397.
[55] Eugene Yakub, Claudio Ronchi, Dragos Staicu, J. Chem. Phys. 127 (2007) 094508.
[56] J.P. Crocombette, F. Jollet, L.T. Nga, T. Petit, Phys. Rev. B 64 (2001) 104107.
[57] J.R. Walker, C.R.A. Catlow, J. Phys. C: Solid State Phys. 14 (1981) L979.
[58] C.R. Catlow, Proc. R. Soc. Lond. A 353 (1977) 533.